university of groningen

University Medical Center Groningen

University of Groningen

Novel imaging aspects in the management of patients with acute coronary syndromes

Wieringa, Wouter

IMPORTANT NOTE: You are advised to consult the publisher's version (publisher's PDF) if you wish to cite from it. Please check the document version below.

Document Version
Publisher's PDF, also known as Version of record

Publication date:
2014

Link to publication in University of Groningen/UMCG research database

Citation for published version (APA):
Wieringa, W. (2014). *Novel imaging aspects in the management of patients with acute coronary syndromes*. [Thesis fully internal (DIV), University of Groningen]. s.n.

Copyright
Other than for strictly personal use, it is not permitted to download or to forward/distribute the text or part of it without the consent of the author(s) and/or copyright holder(s), unless the work is under an open content license (like Creative Commons).

The publication may also be distributed here under the terms of Article 25fa of the Dutch Copyright Act, indicated by the "Taverne" license. More information can be found on the University of Groningen website: https://www.rug.nl/library/open-access/self-archiving-pure/taverne-amendment.

Take-down policy
If you believe that this document breaches copyright please contact us providing details, and we will remove access to the work immediately and investigate your claim.

Downloaded from the University of Groningen/UMCG research database (Pure): http://www.rug.nl/research/portal. For technical reasons the number of authors shown on this cover page is limited to 10 maximum.

Download date: 30-09-2023

In Vivo Differentiation of Coronary Lesions with Noninvasive Computed Tomography Angiography and Invasive Intravascular Ultrasound as Compared to Optical Coherence Tomography

7

Wouter G. Wieringa
Chris P.H. Lexis
Erik Lipsic
Hindrik W. van der Werf
Johannes G.M. Burgerhof
Vincent E. Hagens
G. Louis Bartels
Alexander Broersen
Remco A.J. Schurer
Eng-Shiong Tan
Pim van der Harst
Ad F.M. van den Heuvel
Tineke P. Willems
Gabija Pundziute

Submitted for publication

Abstract

Purpose In vitro studies have shown the feasibility of coronary lesion grading with computed tomography angiography (CTA), intravascular ultrasound (IVUS) and optical coherence tomography (OCT) as compared to histology, whereas OCT had the highest discriminatory capacity. We investigated the ability of CTA and IVUS to differentiate between early and advanced coronary lesions in vivo, OCT serving as the standard of reference.

Methods Multimodality imaging was prospectively performed in 30 patients with NSTEMI. A total of 1083 cross-sections of 30 culprit lesions atherosclerotic plaque characteristics were assessed and co-registered among modalities. Fibrous and fibrocalcific plaque on OCT were defined as early plaque type, whereas lipid rich-plaque on OCT was defined as advanced plaque. To assess associations between each plaque type on CTA and IVUS with early or advanced plaque on OCT, odds ratios (OR) adjusted for clustering were calculated.

Results On cross-sectional level normal findings on CTA as well as on IVUS were associated with early plaque (OR: 0.09; $p<0.001$, and OR: 0.02; $p<0.001$, respectively). Non-calcified plaque on CTA was associated with advanced plaque (OR: 4.04, $p<0.001$) and a trend towards association between advanced plaque and calcified plaque on CTA was observed. The napkin ring sign on CTA was associated with advanced plaque (OR: 4.66, $p<0.001$). On IVUS fatty and calcified plaque were strongly associated with advanced plaque on OCT (OR: 151.93, $p<0.001$).

Conclusions In vivo coronary plaque characteristics on CTA and IVUS are associated with plaque characteristics on OCT. Of note, normal findings on CTA relate to early lesions on OCT. Nevertheless, multiple plaque features on CTA and IVUS are related to advanced plaques on OCT which may make it difficult to use qualitative plaque features to recognize advanced coronary plaques.

Introduction

Rupture of an atherosclerotic plaque with superimposed luminal coronary artery thrombosis is the most common cause of acute coronary events. Coronary artery plaques that are prone to rupture typically contain a large necrotic lipid-rich core and a thin overlying fibrous cap and are often referred to as vulnerable plaques [1-3]. Early detection of vulnerable plaques could potentially prevent coronary events. Computed tomography angiography (CTA) of the coronary arteries is a clinically established tool enabling non-invasive diagnosis of coronary artery disease (CAD) [4]. Besides stenosis assessment, it is possible to assess composition of atherosclerotic plaques with CTA and to a certain extent classify plaques. Although the presence of non-calcified plaque component on CTA was associated with the development of coronary events [5], the knowledge on the ability of CTA to discriminate between components of non-calcified plaque is still limited [6-8].

A multi-modality imaging strategy may enhance our understanding of coronary atherosclerotic lesions that are related to coronary events. Invasive coronary plaque characterization may be performed using intravascular ultrasound (IVUS) and optical coherence tomography (OCT)[9]. Whereas, IVUS is regarded as reference method for coronary plaque dimensions, OCT has shown a high diagnostic accuracy in characterization of plaques, however its penetration depth is limited [10, 11].

The feasibility of coronary lesion grading with CTA, IVUS and OCT as compared to histology was recently elegantly shown in an in vitro setting [12, 13]. OCT yielded the highest discriminatory capacity for advanced plaques as compared to histology [12]. Accordingly, in the study we investigated the ability of CTA and IVUS to differentiate between atherosclerotic plaque characteristics in vivo, with OCT serving as a standard of reference.

Methods

Thirty patients presenting with non-ST-elevation myocardial infarction (NSTEMI) were prospectively included in our study. Inclusion criteria for the study were patients with NSTEMI - chest pain suggestive for myocardial ischemia with typical electrocardiogram changes and a rise of (high sensitivity) troponin T - with a clinical indication for invasive coronary angiography (ICA) followed by reperfusion of the ischemia-related target lesion. Only native coronary artery lesions were included. Exclusion criteria were: persistent ST-segment elevation (>1mm in 2 or more leads), the need for emergency ICA with subsequent PCI or coronary artery bypass grafting (CABG), presence of cardiogenic shock, contraindication to CTA (estimated glomerular filtration rate <50 ml/min, known allergy to iodine contrast agents, cardiac rhythm

other than sinus rhythm, inability to lay supine or sustain a breath-hold for 15 seconds) and no informed consent. Dual-source CTA, IVUS and OCT were performed within 24 hours. The study was approved by the local ethics committee and was carried out according to the Declaration of Helsinki. Written informed consent was obtained from each participant.

Computed tomography angiography

Image acquisition

CTA was performed using a 64-slice dual-source computed tomography scanner (Somatom Definition, Siemens Healthcare, Frochheim, Germany). During CTA acquisition non-ionic contrast medium was administered (Iomeron 400, Bracco, Italy). Beta-blocker treatment (orally or intravenously) and nitroglycerine was administered to achieve optimal image quality. In order to reduce radiation exposure, electrocardiogram-gated current modulation was used in all patients. The following scan parameters were used for the 64-slice dual-source CT scanner: 64 x 2 x 0.6 mm collimation, gantry rotation time of 330 ms, temporal resolution of 83 ms, tube voltage 100 or 120 mV, and maximal tube current of 560 mAs. Upon completion of the scan, images were directly reconstructed in order to achieve motion-free images of the coronary arteries.

Image analysis

Evaluation of CTA images was performed on a remote workstation with dedicated software (QAngio CT, Medis Medical Imaging Systems, Leiden, the Netherlands) [14] in consensus by two experienced observers blinded to other imaging modalities. A predefined window and level setting (window 700 HU, level 200 HU) was used for analysis of lumen and plaque [7]. Display settings were manipulated for optimal analysis of vessel lumen and plaque characteristics, if deemed necessary. Analysis of presence and composition of atherosclerosis were performed on a per segment and on a per cross-section basis. In addition, in all other existing coronary segments the presence and composition of plaque as well as the degree of stenosis were also analyzed. Coronary segments were differentiated into seventeen segments, according to a modified American Heart Association classification [15].

Coronary atherosclerosis was defined as tissue structures >1 mm^2 within or adjacent to the coronary artery lumen but distinctive from surrounding pericardial or epicardial tissue. The degree of luminal narrowing of coronary artery lumen was quantified visually, based on comparison of the luminal diameter of the plaque-containing segment to the luminal diameter of the most normal-appearing site

immediately proximal to the plaque. Plaques with ≥50% luminal narrowing were classified as obstructive. The composition of plaque was classified to one of three types: 1. non-calcified plaque (plaques with lower density compared to contrast-enhanced lumen), 2. calcified plaque (plaques with high density structures compared to contrast-enhanced lumen), or 3. mixed plaque (non-calcified and calcified constituents in single plaque). In addition, the presence of thrombus was assessed on per segment level, which was defined as a homogenous non-calcified structure with irregular borders with a density of <55 HU [16].

On cross-sections with non-calcified plaque component (non-calcified and mixed plaques) the presence of napkin-ring sign (NRS) was scored as a plaque core with low CTA attenuation surrounded by a rim-like area of higher attenuation [17]. Non-calcified and mixed plaques were additionally classified according to their attenuation as low-attenuation (<30 HU) and higher attenuation (≥30HU) plaques [18].

Optical coherence tomography

Image acquisition

The C7 imaging system (St. Jude/LightLab Imaging Inc, MN, USA) was used to perform OCT acquisition. After crossing the culprit lesion with an angioplasty guide wire the OCT catheter (DragonFly catheter, St. Jude Medical/LightLab Imaging Inc, MN, USA) was advanced over the wire and placed distal to the lesion. In order to reduce vasospasm intracoronary nitro-glycerin was administered before OCT acquisition. OCT images were obtained during the intracoronary injection of 13 to 20 ml of contrast medium (Xenetix 300, Guerbet, France) at a rate of 3-4 ml/s and an automatic pullback at a rate of 20 mm/s.

Image analysis

Off-line IVUS and OCT cross-section analyses were performed using dedicated software (QIvus 2.1, Medis medical imaging systems, Leiden, the Netherlands) in consensus by two observers blinded to CTA, IVUS and OCT images of the same patient.

On OCT cross-sections morphological characterization of plaques was performed as follows (19): normal vessel wall; fibrous plaque, homogenous high-backscattering areas; lipid-rich plaque, signal poor regions with diffuse borders in >2 quadrants; fibrocalcific plaque, fibrous plaques with calcific areas (well-delineated, low back-scattering heterogenous regions). Thin cap fibro-atheroma (TCFA) was defined as a lipid-rich plaque with an overlying fibrous cap with a thickness of ≤65 µm (20). When a cross-section showed various plaque types, the most advanced plaque type

was assigned in the following order: lipid-rich plaque > fibrocalcific plaque > fibrous plaque. For comparisons we categorized plaques in early and advanced plaques. Based on associations found in the ex vivo study by Maurovich-Horvat et al. absence of plaque, fibrous and fibrocalcific plaques were defined as early plaques and lipid-rich plaques were defined as advanced plaques [12]. Plaque rupture was identified as the presence of fibrous-cap discontinuity with a cavity formation in the plaque [21]. The presence of thrombus was visually assessed. Intracoronary thrombus was defined as a mass protruding the coronary vessel lumen discontinuous from the vessel wall.

Intravascular ultrasound

Image acquisition

After OCT acquisition, the IVUS catheter (40MHz Atlantis SR pro catheter, Boston Scientific, MA, USA) was advanced to perform IVUS acquisition. The iLab ultrasound imaging system (Boston Scientific, MA, USA) was used to perform IVUS acquisition.

Image analysis

Assessment of IVUS cross-sections was performed in accordance with the working group on intracoronary imaging of the European Society of Cardiology using the following criteria [22]: normal vessel wall, <0.3 mm of intima-media thickness; vessel wall containing plaque, ≥0.3 mm of intima-media thickness; fibrous plaque, >2 quadrants constituted by tissue, with echoreflectivity higher than that of the adventitia; fatty plaque, >2 quadrants constituted by tissue, with echoreflectivity lower than that of the adventitia; fibrocalcific plaque, <2 quadrants of total calcified arc; and calcified plaque, >2 quadrants of total calcific arc.

Image co-registration

Anatomic landmarks, such as side-branches and/or calcifications were used to align CTA, IVUS and OCT images and co-registered cross-sections. Multiplanar CTA reconstructions were created perpendicular to the vessel centerline. At first a visual co-registration was performed to align CTA, IVUS and OCT longitudinal segments. Subsequently, dedicated software (Matcher, Medis Medical Imaging Systems, Leiden, the Netherlands) was used to confirm the performed visual co-registration. Where feasible, the co-registration was revised in order to achieve the best-matched result of the three imaging modalities. Anatomic landmarks were used to match the rotational direction of the cross-sections of CTA, IVUS and OCT.

Statistical analysis

Normally distributed continuous variables are presented as mean±SD. Continuous variables with skewed distribution are presented as medians with 25th and 75th percentile. Categorical variables are presented as numbers and percentages. Group differences were tested using ANOVA test, Pearson χ2, or Fishers exact test where appropriate.

Crude associations of each category of CTA and IVUS with early or advanced plaque defined by OCT were assessed by calculating odds ratios (OR) for each category with the odds of normal plaque serving as reference. An OR >1.0 indicated an increased probability of a lesion being advanced, and an OR <1.0 indicated an increased probability of a lesion being early. Significance of these crude associations was tested using the Fishers exact test. Additionally the associations were recalculated accounting for clustering effect within lesions by using multilevel mixed effect modeling (STATA procedure *xtmelogit*). Bonferroni correction was used because of multiple testing. For each modality the plaque categories were recoded as a new, single variable. For CTA the new variable had three degrees of freedom and for IVUS the new variable had four degrees of freedom. A mixed effects logistic regression for each modality was fitted with the category normal plaque serving as the reference category.

Statistical significance was defined as p-value of <0.05. Statistical analyses were performed using STATA version 11 (College Station, TX, USA).

Results

Study population

A total of thirty patients with NSTEMI were included in the study and multi-modality imaging was performed in 30 culprit lesions.

A total of 1083 cross-sections from 30 culprit segments were available for analysis. The mean number of available cross-sections was 36 per patient. Baseline characteristics of the population are presented in Table 1. The mean age was 68.3 years old, and half were of male gender.

Computed tomography angiography

On lesion level, the majority of the culprit coronary plaques (17; 56.7%) were classified as mixed plaques, whereas 5 (16.6%) were classified as non-calcified plaques and 8 (26.7%) were classified as calcified plaques. Thrombus was scored in 9 (30.0%) of the culprit segments.

On frame level, of the 1083 coronary CTA cross-sections, 257 (23.7%) were classified

Table 1. Patient characteristics

	N = 30
Demographics	
Age (years)	68.3±10.7
Gender (male)	17 (56.7)
Body mass index (kg/m2)	26.8 [24.4-28.9]
Medical history	
Hypertension	16 (53.3)
Diabetes	10 (33.3)
Hypercholesterolaemia	10 (33.3)
Current or previous smoker	13 (43.3)
Family history	8 (26.7)
Previous MI	4 (13.3)
Previous PCI	6 (20.0)
Previous CABG	2 (6.7)
Previous CVA	5 (16.7)
Laboratory values	
CK maximum (mg/L)	164.0 [86.5 - 301.0]
CKMB maximum (mg/L)	21.0 [17.0 - 33.0]
hs-TroponinT maximum (ng/L) [n=9]	192 [51 - 368]
Troponin T maximum (µg/L) [n=21]	0.10 [0.03 - 0.20]
Cholesterol (mmol/L)	4.9 [4.1 - 5.6]
HDL - Cholesterol (mmol/L)	1.4 [1.1 - 1.6]
LDL - Cholesterol (mmol/L)	3.1 [2.2 - 3.4]
Computed Tomography Coronary Angiography characteristics	
Number of segments	15 [14 - 16]
Plaques	8.5 [6.0 - 11.0]
Non-obstructive plaques	6.0 [5.0 - 8.3]
Obstructive plaques	2.0 [1.0 - 3.0]
Non-calcified plaques	1.0 [0 - 1.3]
Mixed plaques	2.0 [0 - 4.0]
Calcified plaques	4.5 [1.0 - 7.0]

The data are mean±SD, median, IQR, or numbers (%). CABG = coronary artery bypass graft; IQR = interquartile range; RCA = right coronary artery; LAD = left anterior descending artery; LCx = left circumflex artery; SD = standard deviation.

as normal, 360 (33.2%) as showing non-calcified plaque, 178 (16.4%) as showing mixed plaque, and 288 (26.7%) as showing calcified plaque. A total of 28/538 (5.2%) cross-sections exhibited a NRS.

Optical coherence tomography

On lesion level, thrombus was detected in 20 (66.7%), plaque rupture in 25 (83.3%), and TCFA in 13 (43.3%) of the culprit lesions.

On frame level, of the 1083 OCT cross-sections, 35 (3.3%) were classified as normal, 296 (27.3%) as fibrous plaques, 467 (43.1%) as fibrocalcific plaques and 285 (26.3%) as lipid-rich plaques. Thrombus was present in 97 (9.0%) frames. TCFA was present in 24 (2.2 %) frames.

Intravascular ultrasound

On lesion level, characteristics visualized by IVUS where as follows: thrombus was detected in 8 (26.7%) culprit segments, and rupture was detected in 13 (43.3%) plaques.

On frame level, of the 1083 IVUS cross-sections, 45 (4.2%) were classified as normal, 380 (35.1%) as fibrous plaques, 369 (34.0%) as fibrocalcific plaques, 173 (16.0%) as calcified plaques, and 116 (10.7%) as fatty plaques. Thrombus was detected in 21 (1.9%) cross-sections.

Table 2. Association between thrombus on OCT and plaque characteristics on coronary CT angiography and IVUS

		Thrombus on OCT	No thrombus on OCT
Segment level		**(n=20)**	**(n=10)**
CT			
	Thrombus	9 (45.0)	0 (0)
	NRS	5 (25.0)	0 (0)
	HU <30	10 (50.0)	1 (10.0)
	Non-calcified	2 (10.0)	3 (30.0)
	Mixed	13 (65.0)	4 (40.0)
	Calcified	5 (25.0)	3 (30.0)
IVUS			
	Thrombus	6 (30.0)	2 (20.0)
Cross-sectional level		**(n=97)**	**(n=986)**
CT			
	Thrombus	20 (20.6)	7 (0.7)
	NRS	16 (16.5)	12 (1.2)
	HU <30	19 (19.6)	11 (1.1)
	Non-calcified	52 (53.6)	308 (31.2)
	Mixed	23 (23.7)	155 (15.7)
	Calcified	22 (22.7)	266 (26.9)
IVUS			
	Thrombus	13 (13.4)	8 (0.8)
	Fibrous	21 (21.7)	359 (36.4)
	Fibrocalcific	31 (31.96)	338 (34.3)
	Calcified	25 (25.8)	148 (15.0)
	Fatty	20 (20.6)	96 (9.7)

The data are numbers (%). CTA = computed tomography angiography; HU = Houndsfield Units; IVUS = intravascular ultrasound; NRS = napkin ring sign; OCT = optical coherence tomography; TCFA = thin-cap fibroatheroma.

Comparison between computed tomography angiography versus optical coherence tomography

On per lesion basis, culprit lesions were grouped based on the presence of thrombus on OCT (Table 2). On CTA, thrombus and NRS were only observed in the groups of lesions with thrombus on OCT, but only in a limited number of lesions. Moreover, limited correlation was observed between the low attenuation value on CTA and the presence of thrombus on OCT. No correlation was observed between the plaque type on CTA and the presence of thrombus. The sensitivity for CTA to detect thrombus was 45% (9/20) and the specificity was 100% (10/10).

On per frame basis, thrombus was visible in only 21% of CTA frames with thrombus on OCT (Table 3). The same limited association was observed between the presence of thrombus on OCT and the NRS and low attenuation plaque.

Normal findings on CTA were associated with early plaque on OCT (Table 4). On the contrary, non-calcified were associated with advanced plaque on OCT and calcified plaques showed trend toward association with advanced plaque. Moreover, NRS was significantly associated with advanced plaque on OCT (OR: 4.66 p<0.001).

Table 3. Plaque composition as assessed at coronary CT angiography and IVUS within atherosclerotic plaque categories as assessed at OCT

	OCT				
	Associated with early lesions				Associated with advanced lesions
Modality and plaque composition	**Normal**	**Fibrous**	**Fibrocalcific**	**Total (all 3)**	**Lipid-rich**
CT					
Normal	23 (9.0)	152 (59.1)	18 (7.0)	193 (75.1)	64 (24.9)
Non-calcified	10 (2.8)	108 (30.0)	106 (29.4)	224 (62.2)	136 (37.8)
Mixed	0 (0)	18 (10.1)	115 (64.6)	133 (74.7)	45 (25.3)
Calcified	2 (0.7)	18 (6.2)	158 (79.2)	248 (86.1)	40 (13.9)
Total	35	296	378	798	285
CT additional information					
Napkin ring sign	0 (0)	1 (3.6)	10 (35.7)	11 (39.3)	17 (60.7)
IVUS					
Normal	30 (66.7)	13 (28.9)	0 (0)	43 (95.6)	2 (4.4)
Fibrous	5 (1.3)	233 (61.3)	51 (13.4)	289 (76.0)	91 (24.0)
Fibrocalcific	0 (0)	44 (11.9)	256 (69.4)	300 (81.3)	69 (18.7)
Calcific	0 (0)	0 (0)	148 (85.5)	148 (85.5)	25 (14.5)
Fatty	0 (0)	6 (5.2)	12 (10.3)	18 (15.5)	98 (84.5)

The data are numbers (%). CTA = computed tomography angiography; HU = Houndsfield Units; IVUS = intravascular ultrasound; OCT = optical coherence tomography.

Table 4. Association of coronary CT angiography and IVUS with lesions on OCT which are associated with early and advanced lesions on histologic examination

Modality and plaque composition		OCT						
		Total	Associated with early lesions	Associated with advanced lesions	Crude analysis		Accounted for clustering	
					OR	p-value	OR	p-value **
CT								
	Normal	257 (23.7)	193 (75.1)	64 (24.9)	0.33*	0.571	0.09*	0.000
	Noncalcified	360 (33.2)	224 (62.2)	136 (37.8)	1.83	0.000	4.04	0.000
	Mixed	178 (16.4)	133 (74.7)	45 (25.3)	1.02	0.780	1.91	0.098
	Calcified	288 (26.6)	248 (86.1)	40 (13.9)	0.49	0.000	2.16	0.049
IVUS								
	Normal	76 (6.6)	43 (95.6)	2 (4.4)	0.05*	0.000	0.02*	0.000
	Fibrous	396 (34.2)	289 (76.0)	91 (24.0)	6.77	0.219	5.61	0.116
	Fibrocalcific	377 (32.6)	300 (81.3)	69 (18.7)	4.94	0.000	6.27	0.087
	Calcific	180 (15.6)	148 (85.5)	25 (14.5)	3.63	0.000	9.47	0.030
	Fatty	128 (11.0)	18 (15.5)	98 (84.5)	117.06	0.000	151.93	0.000

*Odds of the reference category is given
** Bonferroni correction performed
The data are numbers (%). CTA = computed tomography angiography; IVUS = intravascular ultrasound; OCT = optical coherence tomography; OR = odds ratio.

Comparison between grayscale intravascular ultrasound versus optical coherence tomography

On lesion level, a very limited correlation between the presence of thrombus on OCT and IVUS was observed (Table 2). For IVUS the sensitivity and specificity were 30% (6/20) and 80% (8/10), respectively.

On frame level, the correlation between the presence of thrombus on OCT and the findings on IVUS was even lower than on lesion level (Table 2).

Normal findings on IVUS were associated with early plaque on OCT. On the contrary, calcified plaque was associated with advanced plaque on OCT, whereas fatty plaque on IVUS was strongly associated with advanced plaque on OCT (Tables 3 and 4).

An example of findings on all three imaging modalities is presented in Figure 1.

Discussion

In this in vivo study in patients with NSTEMI describing a systematic assessment of coronary lesions using CTA and IVUS compared to OCT as a standard of reference, the findings may be summarized as follows: [1] Normal findings on CTA and IVUS are associated with early plaque as defined by OCT; [2] Non-calcified plaque, NRS and to a lower extent calcified plaque on CTA as well as fatty and calcified plaque on IVUS are significantly associated with advanced plaque as defined by OCT.

In accordance with ex vivo studies, the absence of plaque on CTA was correlated to

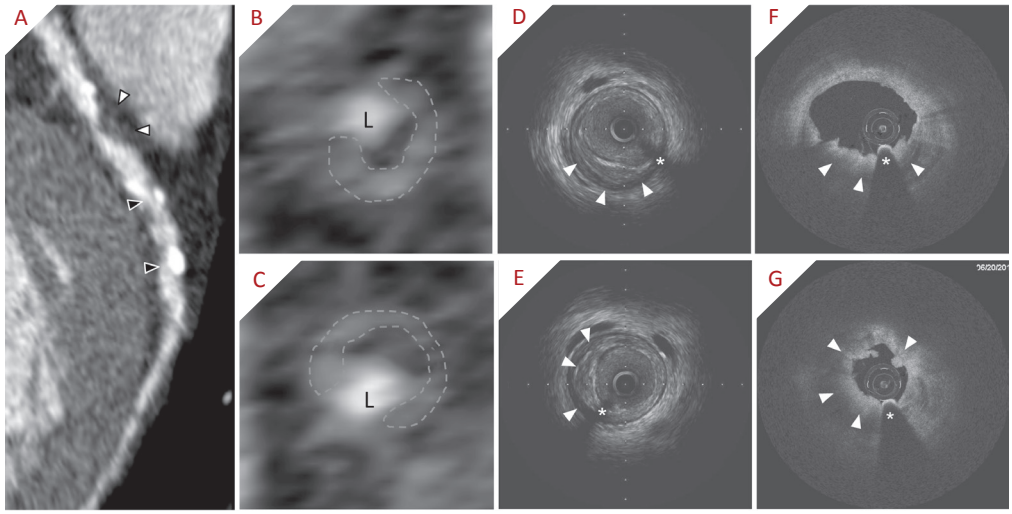

Figure 1. An example of a lesion in left anterior descending artery with corresponding cross-sections on computed tomography, intravascular ultrasound and optical coherence tomography Multiplanar reformatted image of the left anterior descending coronary artery (A) with a mixed plaqe with large non-calcified portion (white arrowheads) and some calcified plaques more distally (black arrowheads). The cross-sectional computed tomography images (B, C) show a coronary plaque with napkin-ring sign attenuation pattern (L = lumen). The circumferential outer rim (dashed blue line) has a higher contrast attenuation as compared to the inner part of the plaque. Intravascular ultrasound (D, E) images show a predominantly fibrous plaque (white arrowheads). Optical coherence tomography (F, G) of the corresponding cross-sections shows (mural) thrombus in both positions (white arrowheads).
* represents the shadow of the guidewire.

early plaque on OCT [12, 13]. Indeed, Maurovich-Horvath et al. have recently observed in an experimental model that normal findings by CTA were strongly associated with early atherosclerotic plaque on histological examination (OR: 0.02; p<0.001) [12]. The finding is line with prospective clinical studies which have shown that the absence of CAD on CTA resulted in no coronary events during follow-up [23-25]. This finding further supports the application of coronary CTA for exclusion of CAD. Moreover, correlation between certain coronary plaque characteristics on CTA and advanced lesions on OCT has been observed. A significant correlation between non-calcified plaque on CTA and advanced plaque on OCT has been found in our dataset, which is contrary to the findings in the previous ex vivo study where correlation between advanced lesions on histology and mixed plaque on CTA was observed [12]. From a clinical point of view both types of plaques (non-calcified and mixed) were related to coronary events on follow-up [5, 23, 26-28]. Moreover, the difference in the findings may be related to the different reference standard used in our study (OCT versus histopathology). Another interesting observation is the correlation between the NRS on CTA and advanced coronary plaque. Previous studies have shown the relation between the NRS and high-risk coronary plaques [13, 29-31]. In a study with donor hearts the specificity of NRS to identify histopathologically advanced lesions and TCFA was as high as 99% [13]. Moreover, another study demonstrated that the presence of NRS within a coronary

plaque is strongly associated with future cardiac events independent of other high-risk CTA features, such as positive remodeling and low attenuation plaque [32]. Nevertheless, we have also observed a trend toward correlation between advanced lesions on OCT and calcified plaque on CTA. The same finding has been reported in a study by Maurovich-Horvat et al.[13]. Since multiple coronary plaque features are related to advanced coronary lesions on OCT or histology as a standard of reference, it may be difficult to use qualitative coronary plaque features on CTA for further risk stratification.

Similar correlations between coronary plaque features and OCT were observed also on IVUS. Indeed, normal findings on IVUS were related to early lesions on OCT, whereas a strong correlation between the fatty plaque on IVUS and advanced plaque on OCT was observed. Also, similar to the findings on CTA calcified plaque on IVUS was related to advanced lesions. The findings are somewhat discrepant from the findings in a previous ex vivo study [12], which could be related to different classification scheme applied in our study and a small sample size.

In the present study we also assessed the ability of CTA and IVUS with inferior spatial resolution as compared to OCT to characterize non-calcified plaque component, including the assessment of thrombus. Thrombus was present in 66.7% of culprit lesions evaluated with OCT, which corresponds well to the prevalence of thrombus in culprit lesions of NSTEMI patients using OCT (65 – 68%) [33, 34]. Nevertheless, thrombus could only be identified in 30% of culprit lesions on IVUS. Our results correspond with the findings by Kubo et al., who reported the diagnostic accuracy for detection of thrombus by IVUS to be as low as 33% as compared to OCT and coronary angioscopy [21]. Regarding CTA, there are only a few reports available on the detection of coronary thrombus [16]. As expected, the accuracy of thrombus detection on CTA in our study was as low as 45%. Moreover, no other plaque features were associated with intracoronary thrombus on IVUS and CTA either on segmental or frame level (Table 2), which further emphasizes the limitation of IVUS and CTA to characterize non-calcified tissue. Accordingly, the presence of thrombus on IVUS and CTA should be interpreted with caution.

Our results should be interpreted in the context of several limitations. First, an important limitation of this study is the lack of histopathological data, however this study was designed as an in vivo study. Second, as the used modalities are different from the technical point of view, the plaque classification schemes were also different. Therefore direct comparison of plaque characteristics was difficult to perform. Finally, performing a complex multi-modality imaging study is difficult due to the costs and logistical difficulties. Therefore only a small number of patients could

be recruited to participate in the study resulting in a limited sample size.

In conclusion, in vivo coronary plaque characteristics on CTA and IVUS are associated with plaque characteristics on OCT. Of note, normal findings on CTA relate to early lesions on OCT. Nevertheless, multiple plaque features on CTA and IVUS are related to advanced plaques on OCT which may make it difficult to use qualitative plaque features to recognize advanced coronary plaques in clinical practice. Future studies in bigger samples are necessary to confirm the findings.

References

1. Kolodgie FD, Burke AP, Farb A, et al. The thin-cap fibroatheroma: a type of vulnerable plaque: the major precursor lesion to acute coronary syndromes. Curr Opin Cardiol 2001;16(5):285-292.

2. Falk E, Nakano M, Bentzon JF, Finn AV, Virmani R. Update on acute coronary syndromes: the pathologists' view. Eur Heart J 2013;34(10):719-728.

3. Virmani R, Kolodgie FD, Burke AP, Farb A, Schwartz SM. Lessons from sudden coronary death: a comprehensive morphological classification scheme for atherosclerotic lesions. Arterioscler Thromb Vasc Biol 2000;20(5):1262-1275.

4. Voros S, Rinehart S, Qian Z, et al. Coronary atherosclerosis imaging by coronary CT angiography: current status, correlation with intravascular interrogation and meta-analysis. JACC Cardiovasc Imaging 2011;4(5):537-548.

5. van Werkhoven JM, Schuijf JD, Gaemperli O, et al. Incremental prognostic value of multi-slice computed tomography coronary angiography over coronary artery calcium scoring in patients with suspected coronary artery disease. Eur Heart J 2009;30(21):2622-2629.

6. Achenbach S, Moselewski F, Ropers D, et al. Detection of calcified and noncalcified coronary atherosclerotic plaque by contrast-enhanced, submillimeter multidetector spiral computed tomography: a segment-based comparison with intravascular ultrasound. Circulation 2004;109(1):14-17.

7. Leber AW, Knez A, Becker A, et al. Accuracy of multidetector spiral computed tomography in identifying and differentiating the composition of coronary atherosclerotic plaques: a comparative study with intracoronary ultrasound. J Am Coll Cardiol 2004;43(7):1241-1247.

8. Pohle K, Achenbach S, Macneill B, et al. Characterization of non-calcified coronary atherosclerotic plaque by multi-detector row CT: comparison to IVUS. Atherosclerosis 2007;190(1):174-180.

9. Kawasaki M, Bouma BE, Bressner J, et al. Diagnostic accuracy of optical coherence tomography and integrated backscatter intravascular ultrasound images for tissue characterization of human coronary plaques. J Am Coll Cardiol 2006;48(1):81-88.

10. Mintz GS, Nissen SE, Anderson WD, et al. American College of Cardiology Clinical Expert Consensus Document on Standards for Acquisition, Measurement and Reporting of Intravascular Ultrasound Studies (IVUS). A report of the American College of Cardiology Task Force on Clinical Expert Consensus Documents. J Am Coll Cardiol 2001;37(5):1478-1492.

11. Yabushita H, Bouma BE, Houser SL, et al. Characterization of human atherosclerosis by optical coherence tomography. Circulation 2002;106(13):1640-1645.

12. Maurovich-Horvat P, Schlett CL, Alkadhi H, et al. Differentiation of early from advanced coronary atherosclerotic lesions: systematic comparison of CT, intravascular US, and optical frequency domain imaging with histopathologic examination in ex vivo human hearts. Radiology 2012;265(2):393-401.

13. Maurovich-Horvat P, Schlett CL, Alkadhi H, et al. The napkin-ring sign indicates advanced atherosclerotic lesions in coronary CT angiography. JACC Cardiovasc Imaging 2012;5(12):1243-1252.

14. Boogers MJ, Schuijf JD, Kitslaar PH, et al. Automated quantification of stenosis severity on 64-slice CT: a comparison with quantitative coronary angiography. JACC Cardiovasc Imaging 2010;3(7):699-709.

15. Austen WG, Edwards JE, Frye RL, et al. A reporting system on patients evaluated for coronary artery disease. Report of the Ad Hoc Committee for Grading of Coronary Artery Disease, Council on Cardiovascular Surgery, American Heart Association. Circulation 1975;51(4 Suppl):5-40.

16. Achenbach S, Marwan M. Intracoronary thrombus. J Cardiovasc Comput Tomogr 2009;3(5):344-345.

17. Maurovich-Horvat P, Hoffmann U, Vorpahl M, Nakano M, Virmani R, Alkadhi H. The napkin-ring sign: CT signature of high-risk coronary plaques? JACC Cardiovasc Imaging 2010;3(4):440-444.

18. Motoyama S, Kondo T, Anno H, et al. Atherosclerotic plaque characterization

by 0.5-mm-slice multislice computed tomographic imaging. Circ J 2007;71(3):363-366.

19. Tearney GJ, Regar E, Akasaka T, et al. Consensus standards for acquisition, measurement, and reporting of intravascular optical coherence tomography studies: a report from the International Working Group for Intravascular Optical Coherence Tomography Standardization and Validation. J Am Coll Cardiol 2012;59(12):1058-1072.

20. Kume T, Akasaka T, Kawamoto T, et al. Measurement of the thickness of the fibrous cap by optical coherence tomography. Am Heart J 2006;152(4):755.e1-755.e4.

21. Kubo T, Imanishi T, Takarada S, et al. Assessment of culprit lesion morphology in acute myocardial infarction: ability of optical coherence tomography compared with intravascular ultrasound and coronary angioscopy. J Am Coll Cardiol 2007;50(10):933-939.

22. Di Mario C, Gorge G, Peters R, et al. Clinical application and image interpretation in intracoronary ultrasound. Study Group on Intracoronary Imaging of the Working Group of Coronary Circulation and of the Subgroup on Intravascular Ultrasound of the Working Group of Echocardiography of the European Society of Cardiology. Eur Heart J 1998;19(2):207-229.

23. Pundziute G, Schuijf JD, Jukema JW, et al. Prognostic value of multislice computed tomography coronary angiography in patients with known or suspected coronary artery disease. J Am Coll Cardiol 2007;49(1):62-70.

24. Min JK, Shaw LJ, Devereux RB, et al. Prognostic value of multidetector coronary computed tomographic angiography for prediction of all-cause mortality. J Am Coll Cardiol 2007;50(12):1161-1170.

25. Hadamitzky M, Freissmuth B, Meyer T, et al. Prognostic value of coronary computed tomographic angiography for prediction of cardiac events in patients with suspected coronary artery disease. JACC Cardiovasc Imaging 2009;2(4):404-411.

26. Motoyama S, Sarai M, Harigaya H, et al. Computed tomographic angiography characteristics of atherosclerotic plaques subsequently resulting in acute coronary syndrome. J Am Coll Cardiol 2009;54(1):49-57.

27. Motoyama S, Kondo T, Sarai M, et al. Multislice computed tomographic characteristics of coronary lesions in acute coronary syndromes. J Am Coll Cardiol 2007;50(4):319-326.

28. Russo V, Zavalloni A, Bacchi Reggiani ML, et al. Incremental prognostic value of coronary CT angiography in patients with suspected coronary artery disease. Circ Cardiovasc Imaging 2010;3(4):351-359.

29. Kashiwagi M, Tanaka A, Kitabata H, et al. Feasibility of noninvasive assessment of thin-cap fibroatheroma by multidetector computed tomography. JACC Cardiovasc Imaging 2009;2(12):1412-1419.

30. Tanaka A, Shimada K, Yoshida K, et al. Non-invasive assessment of plaque rupture by 64-slice multidetector computed tomography--comparison with intravascular ultrasound. Circ J 2008;72(8):1276-1281.

31. Nakazawa G, Tanabe K, Onuma Y, et al. Efficacy of culprit plaque assessment by 64-slice multidetector computed tomography to predict transient no-reflow phenomenon during percutaneous coronary intervention. Am Heart J 2008;155(6):1150-1157.

32. Otsuka K, Fukuda S, Tanaka A, et al. Napkin-ring sign on coronary CT angiography for the prediction of acute coronary syndrome. JACC Cardiovasc Imaging 2013;6(4):448-457.

33. Toutouzas K, Karanasos A, Tsiamis E, et al. New insights by optical coherence tomography into the differences and similarities of culprit ruptured plaque morphology in non-ST-elevation myocardial infarction and ST-elevation myocardial infarction. Am Heart J 2011;161(6):1192-1199.
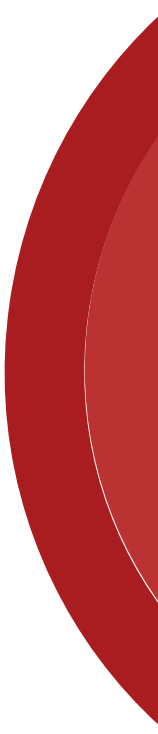
34. Ino Y, Kubo T, Tanaka A, et al. Difference of culprit lesion morphologies between ST-segment elevation myocardial infarction and non-ST-segment elevation acute coronary syndrome: an optical coherence tomography study. JACC Cardiovasc Interv 2011;4(1):76-82.